0026-895X/97/020328-08$3.00/0

MOLECULAR PHARMACOLOGY, **51:**328–335 (1997).

# Contrasting Actions of Lanthanum on Different Recombinant γ-Aminobutyric Acid Receptor Isoforms Expressed in L929 Fibroblasts

NINA C. SAXENA,[1] TORBEN R. NEELANDS, and ROBERT L. MACDONALD

*Departments of Neurology (N.C.S., T.R.N.) and Physiology (R.L.M.), University of Michigan Medical School, Ann Arbor, Michigan 48104-1687*

Received August 1, 1996; Accepted October 31, 1996

**SUMMARY**

Functional studies have indicated that, unlike most divalent cations, lanthanum increases both native and recombinant γ-aminobutyric acid (GABA) receptor (GABAR) currents. In the present study, we have examined whether lanthanum shows subunit-dependent selectivity for modification of currents from different GABAR isoforms. The effects of lanthanum on three different GABAR isoforms, $\alpha1\beta3\gamma2L$, $\alpha6\beta3\gamma2L$, and $\alpha6\beta3\delta$, were determined by transient expression of combinations of $\alpha1$, $\alpha6$, $\beta3$, $\gamma2L$, and $\delta$ subunit cDNAs in L929 fibroblasts. Whole-cell recording was used to determine the concentration-response curves for lanthanum for the three different isoforms at submaximal concentrations of GABA. Lanthanum displayed strong potentiation of $\alpha1\beta3\gamma2L$ GABAR currents consistent with earlier reports of potentiation of GABAR currents by lanthanum in neurons and recombinant GABAR isoforms. However, in contrast to the potentiation of $\alpha1\beta3\gamma2L$ GABAR currents by lanthanum, $\alpha6\beta3\delta$ GABAR currents were strongly inhibited and $\alpha6\beta3\gamma2L$ GABAR currents were weakly inhibited by lanthanum. Interaction of lanthanum with GABAR isoforms was competitive, with lanthanum decreasing the $EC_{50}$ value for GABA of $\alpha1\beta3\gamma2L$ GABARs without changing the maximum current and increasing the $EC_{50}$ value for GABA of $\alpha6\beta3\delta$ and $\alpha6\beta3\gamma2L$ GABAR currents (greater shift in $EC_{50}$ value in the $\alpha6\beta3\delta$ compared with the $\alpha6\beta3\gamma2L$ GABARs) without changing the maximum GABAR current. Neither potentiation nor inhibition of GABAR currents by lanthanum showed any voltage dependence. These results suggest that 1) changing the α-subunit subtype from α1 to α6 altered the effect of lanthanum from potentiation to inhibition, 2) changing the γ2L subunit to the δ-subunit changed the level of maximal inhibition of α6 subtype-containing GABAR currents by lanthanum, and 3) the site for interaction with lanthanum probably was on the extracellular surface of GABARs.

Lanthanum is a trivalent cation and is the most electropositive element of the rare earth group. Its mechanisms of action at the cellular and molecular level have not been studied extensively until recently. Functional studies have indicated that lanthanum, unlike most divalent cations, increases GABA-activated currents in both native and recombinant GABARs (1–4). Based on earlier studies suggesting that changes in subunit composition produced recombinant receptors with differential selectivity toward benzodiazepines and the divalent cation zinc, we formulated this study to determine whether lanthanum displays similar subunit-dependent selectivity toward different GABAR isoforms. There is considerable interest in the effects of lanthanum and its compounds on cellular systems from a neurotoxicological point of view due to its increasing use in industry and therapeutics (5). There is evidence in cell culture and animal systems to suggest that micromolar concentrations of lanthanum can exert cytotoxic effects (6). Study of the cytotoxicity of lanthanum chloride in a pulmonary macrophage primary culture system indicated an half-maximum lethal concentration of 52 μM (7). Traces of lanthanum (0.5 μg/g) were detected in the bones of man and animals after exposure (8). More recent studies of autopsy specimens from deceased smelter factory workers exposed to lanthanum have indicated a 2- to 16-fold increase in lanthanum levels, compared with nonexposed controls; lanthanum levels were highest in those who died of lung cancer (5).

A number of different approaches have been taken to understand the mechanism of action of lanthanum and other heavy metals. Behavioral, anatomical, and biochemical approaches have been useful in identifying the overall toxic effects, structural changes in various regions of the nervous system and biochemical modifications caused by toxicants. However, functional studies using electrophysiological tech-

[1] Current affiliation: Department of Physiology, Emory University, Atlanta, GA 30322.

This work was supported by a Grant NS33300 from the National Institute for Neurological Disorders and Stroke (R.L.M.).

**ABBREVIATIONS:** GABA, γ-aminobutyric acid; GABAR, $GABA_A$ receptor; PBS, phosphate-buffered saline; FDG, fluorescein di-β-galactopyranoside; HEPES, 4-(2-hydroxyethyl)-1-piperazineethanesulfonic acid; EGTA, ethylene glycol bis(β-aminoethyl ether)-*N*,*N*,*N*′,*N*′-tetraacetic acid.

niques could provide information about the cellular and molecular mechanisms of action of heavy metals and suggest how they alter the excitability of the nervous system and lead to behavioral changes (4). In the present study, we have compared and contrasted the effects of lanthanum on the electrophysiological properties of three different putative cerebellar GABAR isoforms transiently expressed in L929 fibroblasts using the whole-cell recording configuration. Specifically, we have examined the effects of changes in subunit subtype composition (among the three GABAR isoforms) on the nature and extent of modulation of GABAR currents by lanthanum. Our results demonstrate GABAR subunit-dependent actions of lanthanum.

## Materials and Methods

**Plasmid construction.** Full-length cDNAs encoding the rat $\alpha$1, $\beta$3, and $\delta$ GABAR subunits were kindly provided by Dr. A. J. Tobin ($\alpha$1; University of California, Los Angeles), Dr. D. B. Pritchett ($\beta$3; University of Pennsylvania, Philadelphia, PA) and Dr. K. Angelides ($\delta$; Baylor College of Medicine, Houston, TX) in the bluescript vector. The rat $\gamma$2L and $\alpha$6 subunits were cloned in our laboratory by Fang Tan (University of Michigan, Ann Arbor, MI). The rat cDNAs have been described previously (see Ref. 9 for review). The plasmids were cut with appropriate restriction enzymes to release the complete open reading frames and 10–100 bp of the 5′ and 3′ untranslated regions, including the Kozak sequences (10, 11). These plasmids were subcloned individually into the *Bgl*II site of the mammalian expression vector pCMVNeo (12) to form the plasmids pCMVr$\alpha$1, pCMVr$\alpha$6, pCMVr$\beta$3, pCMVr$\gamma$2L, and pCMVr$\delta$. A 3000 bp *Bgl*II fragment of pSV$_2\beta$gal [obtained from Dr. Audrey Seasholtz (University of Michigan, Ann Arbor, MI) (13)] was subcloned into pCMVNeo to create the vector pCMV$\beta$gal.

**Preparation of gridded dishes.** Individual 35-mm tissue culture dishes (Corning Glassworks, Corning, NY) were imprinted with a 26 × 26 grid (300 $\mu$m per grid edge) on the bottom with a Mecanex BB form 2 device (Medical Systems, Greenvale, NY) according to the manufacturer's instructions. After plating at low density, cells could be accurately located relative to a particular grid, identified by a corresponding two-letter alphabetic code, while switching between the fluorescent and the electrophysiology microscopes. The process of imprinting the grid removed some of the negative charges required for cell adherence, necessitating a coating of one or two drops of collagen (0.5 mg/ml) in PBS for optimal adherence of L929 cells. The gridded region of the dish was coated with collagen and UV-sterilized overnight before cells were plated on it.

**Cell culture and DNA transfection.** L929 cells were grown in Dulbecco's modified Eagle's medium with 10% horse serum along with 100 IU/ml of penicillin and 100 $\mu$g/ml of streptomycin at 37° in 5% $CO_2$/95% air. Cells were passaged the night before they were to be transfected with trypsin/EDTA solution (0.5% and 0.2%, respectively) and plated at 70% confluency (500,000 cells per 60-mm dish) in a 60-mm dish. The next day, cells were transfected with various combinations of CsCl-banded pCMVr$\alpha$1, pCMVr$\alpha$6, pCMVr$\beta$3, pCMVr$\gamma$2L, pCMVr$\delta$, and pCMVr$\beta$gal plasmids, using a modified calcium phosphate precipitation method (14). Plasmids were mixed in a 1:1:1 ($\alpha$:$\beta$:$\beta$gal) or 1:1:1:1 ($\alpha$:$\beta$:$\gamma$:$\beta$gal or $\alpha$:$\beta$:$\delta$:$\beta$gal) ratio while maintaining the total amount of DNA added per dish at 16–20 $\mu$g in 500 $\mu$l of transfection buffer. Cells were shocked with a 15% glycerol/1 × PBS solution for 30 sec, 4 or 5 hr after the addition of precipitate. Cells were passaged as above 24 hr after addition of precipitate and placed in 15-ml conical tubes and treated with 375 $\mu$g/ml tissue culture grade DNase I for 5 min (twice, for a total time of treatment with DNase I of 10 min) at 37°. Cells were pelleted at 400 × $g$ and plated onto either standard 35-mm plates or mecanex-gridded plates. Electrophysiological analysis was performed 24 hr later.

**Galactosidase staining protocols.** Two different $\beta$-galactosidase staining protocols were used to identify cells transfected with pCMV$\beta$gal. To determine the transfection efficiency, 5-bromo-4-chloro-3-indoyl $\beta$-D-galactosidase staining of cells was performed as described previously (15). FDG staining was performed as originally described by Nolan *et al.* (16), with some modifications for use with adherent cells, to identify positively transfected cells for electrophysiological recordings. Cells were washed twice with PBS to remove the medium and incubated for 5 min at 37° with 1 ml of PBS to re-equilibrate the cells to this temperature. While the cells were incubating, 20 mM FDG solution prepared by the manufacturer (Molecular Probes, Eugene, OR) was diluted 1:20 by adding 25 $\mu$l of the 20 mM FDG solution into 500 $\mu$l of 0.5 × PBS in a 1.5-ml microcentrifuge tube and placed in a 37° water bath. After 5 min of incubation, PBS was aspirated from the cells, and the warmed 1-mM FDG solution (final concentration) was added to the cells. The plate with the cell and FDG solution was warmed in the 37° water bath for 1 min, placed on ice, and then 2.5 ml of ice-cold 1 × PBS was added. After 5 min on ice, the cells were viewed with a fluorescence microscope fitted with fluorescein filters.

**Recording solutions and electrodes.** Before recording, the PBS/FDG solution on the plate of cells was exchanged with five 2-ml washings of external recording medium containing the following: 142 mM NaCl, 8.1 mM KCl, 6 mM $MgCl_2$, 1 mM $CaCl_2$, 10 mM glucose, 10 mM HEPES, pH ~7.4. The internal (intrapipette) solution contained 153 mM KCl, 1 mM $MgCl_2$, 5 mM EGTA, 10 mM HEPES, pH ~7.3. This combination of external and intrapipette solutions produced a chloride equilibrium potential of −1.4 mV and a potassium equilibrium potential of −75 mV across the patch membrane. GABA was diluted with external recording solution from a stock solution (100 mM or 10 mM in distilled water) to the indicated final concentration on the day of the experiment. A multipuffer application system (50–90 $\mu$m tip diameter) was used to apply a range of different concentrations of drugs for experiments.

Micropipettes and recording electrodes were fabricated on a Flaming Brown micropipette puller (Model P-87; Sutter Instruments). Microhematocrit capillary tubes made of sodalime glass (i.d., 1.1–1.2 mm; absorbance, 1.3–1.4 mm; Fisher Scientific, Pittsburgh, PA) were used to fabricate the recording electrodes; a type of borosilicate glass with filament (absorbance, 1.2 mm; World Precision Instruments, New Haven, CT) and a pyrex, nonfilament custom glass tubing (i.d., 0.6 mm; absorbance, 1.2 mm; Drummond Scientific Co., Broomall, PA) were used for the pressure ejection micropipettes and a multipuffer application system, respectively. Recording electrodes were coated with Q-Dope before use and had resistances ranging from 5 to 10 MΩ when filled with the internal solution and immersed in a dish containing the external solution.

**Multipuffer system to apply a range of different concentrations of drugs.** To enable fast application of a number of different concentrations and types of drug, a multipuffer application system was designed in the laboratory (17). Briefly, it consisted of a T-tube device with inlet and outlet ports feeding into a common application port at one end and individually connected to polyethylene tubing leading to either a reservoir of different solutions to be tested (inlet tubing) or the waste flask (outlet tubing) at the other end. Puffer tips between 50 and 90 $\mu$m in diameter made of nonfilament glass were inserted into the application port. A suction pump (aquarium air pump; Supra, Oakland, NJ) was connected to the outlet tubing of the U-tube device via a three-way miniature solenoid valve (General Valve, Fairfield, NJ) operated by a valve driver (Valve driver II; General Valve). To apply a drug, the valve was turned off (regulated by timer), stopping the suction of solution through the U-tube device and pushing the resultant column of accumulated solution in the application port out through the puffer tip. Reactivation of the valve resumed flow of solution through the U tube and suction of the applied drug/solution from the bath, thus affecting a washout of the drug from the area around the puffer tip and cell. The multipuffer application system was tested for a satisfactory rate of application

and removal of drug from the bath before every experiment using the dye, fast green (Sigma Chemical, St. Louis, MO) in a petri dish filled with distilled water. The rate of application and removal of the solutions depended on the size of the tip and its position relative to the cell [$\tau$ between 30 and 70 msec, measuring tip potential between potassium-free (0 mM KCl) and potassium-containing (120 mM KCl) solutions].

**Whole-cell recordings and analyses.** Whole-cell recording was performed with methods described previously for mouse spinal cord neuron recordings (18, 19) using a List L/M EPC-7 amplifier (List Electronics, Darmstadt, Germany). All recordings were made at room temperature (22–24°). Currents were recorded simultaneously on a video cassette recorder (Sony SL-HF360; Sony, Tokyo, Japan) via a digital audio processor (Sony PCM-501 ES, 14-bit, 44 kHz), on Axotape (Version 2; Axon Instruments, Burlingame, CA; using an Axon TL-1–40 16-channel, 40-kHz, 12-bit interface) on a IBM-compatible 80286 personal computer and a chart recorder (Gould, Cleveland, OH) for later computer analysis. Whole-cell recordings were low-pass filtered (3 db at 1 kHz, 8-pole Bessel filter; Frequency Devices, Haverhill, MA) before the chart recorder. The peak whole-cell current amplitudes were measured either using Axotape or directly from the chart output and reported as mean ± standard error. Statistical tests of significance were performed using paired Student's $t$ test for all drug treatments and the $p$ values were reported. Concentration response curves were fitted to a four-parameter logistic function $R = R_{min} + (R_{max} - R_{min})/(1 + 10)^{\text{Log EC}_{50} - X)n)}$, where $X$ is logarithm of drug concentration, $R$ is the response to drug, $R_{max}$ is the maximum drug response, $R_{min}$ is the minimum drug response, Log $EC_{50} = X$ value when the response is halfway between maximum and minimum, and $n$ is the Hill slope, a unitless variable that controls the slope of the curve (Prism; GraphPAD Software, San Diego, CA).

## Results

**GABA responsiveness of transfected L929 cells.** Previous work from our laboratory has shown that six putative cerebellar GABAR isoforms, $\alpha1\beta3\gamma2L$, $\alpha1\beta2\gamma2L$, $\alpha6\beta3\gamma2L$, $\alpha6\beta2\gamma2L$, $\alpha6\beta3\delta$, and $\alpha1\beta2\gamma L$ GABARs, show high levels of functional expression after transient transfection in mouse fibroblast L929 cells (20). Concentration response curves for GABA corresponding to $\alpha1\beta3\gamma2L$, $\alpha6\beta3\gamma2L$, and $\alpha6\beta3\delta$ GABAR isoforms showed typical sigmoidal shapes with different $EC_{50}$ values for GABA and maximal GABA-evoked current amplitudes. The $\alpha6\beta3\delta$ GABARs displayed an $EC_{50}$ value of 0.3 $\mu$M and a maximum current amplitude of 371 ± 116 pA (eight experiments), the $\alpha6\beta3\gamma2L$ GABARs showed an $EC_{50}$ value of 2 $\mu$M and a maximum current amplitude of 730 ± 305 pA (nine experiments), and the $\alpha1\beta3\gamma2L$ GABARs exhibited an $EC_{50}$ value of 14 $\mu$M and a maximum current amplitude of 803 ± 141 pA (nine experiments) (20).

**Modulation of GABAR currents by the polyvalent cation lanthanum.** To determine the effect of lanthanum on the three putative cerebellar GABAR isoforms, we examined the effect of 300 $\mu$M lanthanum on GABA-evoked $\alpha6\beta3\delta$, $\alpha6\beta3\gamma2L$, and $\alpha1\beta3\gamma2L$ whole-cell currents at submaximal concentrations of GABA (close to the respective $EC_{50}$ values for GABA). The concentrations used were 0.3, 3, and 10 $\mu$M GABA for the $\alpha6\beta3\delta$, $\alpha6\beta3\gamma2L$, and $\alpha1\beta3\gamma2L$ GABAR isoforms, respectively (Fig. 1). 300 $\mu$M lanthanum enhanced 10 $\mu$M GABA-evoked $\alpha1\beta3\gamma2L$ currents to 145 ± 12% (mean ± standard error, $n = 8$) of the control current evoked by GABA alone. In contrast, it did not potentiate $\alpha6\beta3\gamma2L$ and $\alpha6\beta3\delta$ GABAR currents, blocking $\alpha6\beta3\gamma2L$ currents by 30 ± 10% (mean ± standard error, $n = 8$) and $\alpha6\beta3\delta$ currents by 81 ± 5% (mean ± standard error, $n = 8$) (Fig. 2).

To further characterize the differential modulation by lanthanum of $\alpha1\beta3\gamma2L$, $\alpha6\beta3\gamma2L$, and $\alpha6\beta3\delta$ GABAR currents, concentration response curves for lanthanum were obtained at submaximal concentrations of GABA. The current amplitudes were expressed as percentages of the current evoked by GABA in the absence of lanthanum. The concentration response curves for lanthanum were fitted using a four-parameter logistic equation (Prism, GraphPAD Software; see eq. 1).

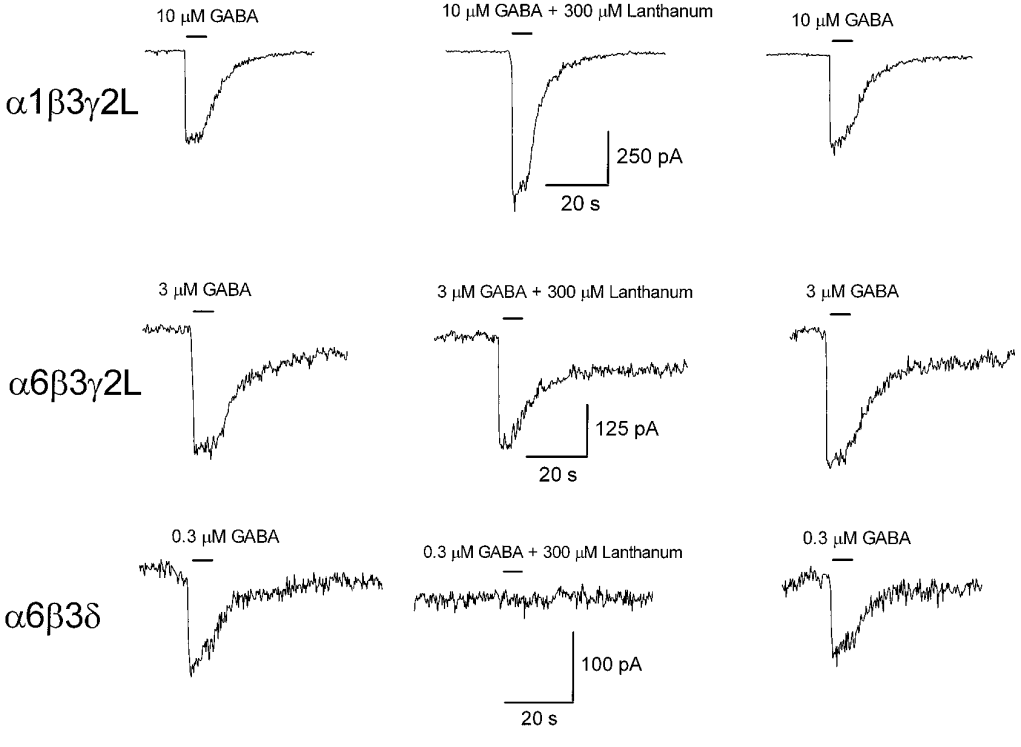


**Fig. 1.** Effect of 300 $\mu$M lanthanum on GABA-evoked whole-cell currents recorded from L929 cells transfected with $\alpha1\beta3\gamma2L$, $\alpha6\beta3\gamma2L$, and $\alpha6\beta3\delta$ GABAR subtypes. Cells were voltage-clamped at −75 mV, and 5-sec pulses of submaximal concentrations of GABA with and without 300 $\mu$M lanthanum were applied via pressure-ejection micropipette placed close to the cells. *Downward deflections*, inward currents (efflux of negatively charged chloride ions) at −75 mV ($E_{Cl}$ = 0 mV). *Horizontal bars above the current traces*, the duration of application of GABA. The recovery of current amplitudes after washout of lanthanum to pretreatment values indicates reversibility of the effect of lanthanum.

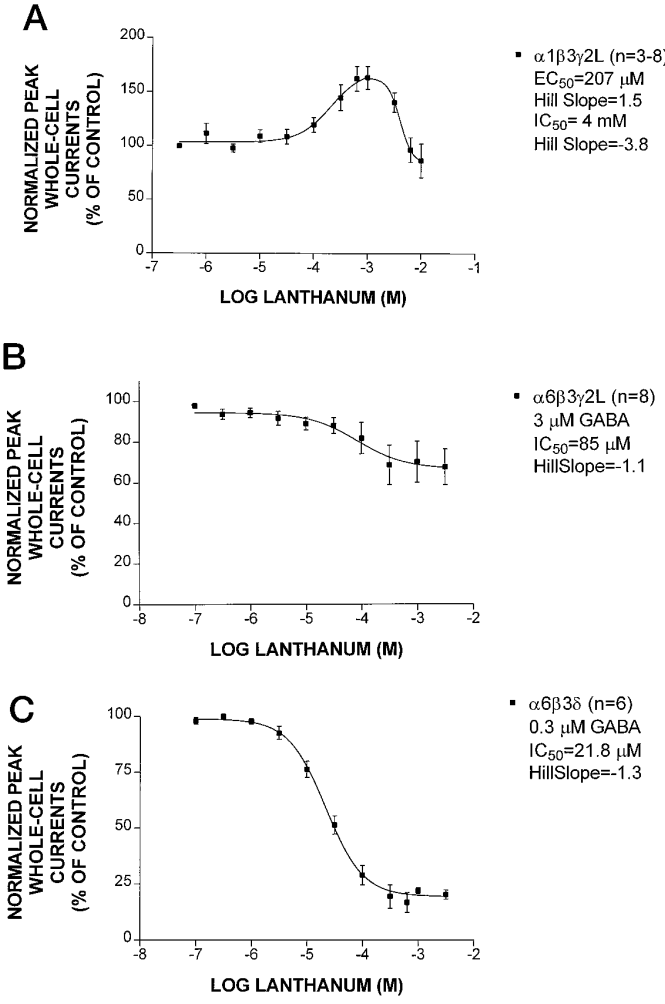


**Fig. 2.** Normalized concentration-response curves for lanthanum corresponding to cells transfected with $\alpha1\beta3\gamma2L$ (A), $\alpha6\beta3\gamma2L$ (B), and $\alpha6\beta3\delta$ (C) GABAR subtypes. *Symbols*, mean values of current amplitudes as a percent of maximum current induced by 10, 3, and 0.3 $\mu$M GABA for the $\alpha1\beta3\gamma2L$ ($n = 4$), $\alpha6\beta3\gamma2L$ ($n = 8$), and $\alpha6\beta3\delta$ ($n = 8$) GABAR isoforms, respectively, in the absence of lanthanum. *Vertical bars*, mean ± standard error.

Normalized current amplitudes were plotted as a function of increasing concentrations of lanthanum (Fig. 2). Lanthanum (1 mM) potentiated $\alpha1\beta3\gamma2L$ GABAR currents to a maximum of 164 ± 11% ($n = 8$, $p < 0.001$) of control current in the absence of lanthanum with an $EC_{50}$ value of 210 ± 61 $\mu$M and Hill slope of 1.5. In contrast to the potentiation of $\alpha1\beta3\gamma2L$ GABAR currents by lanthanum, the $\alpha6\beta3\delta$ GABAR currents were strongly inhibited and $\alpha6\beta3\gamma2L$ GABAR currents were weakly inhibited by lanthanum. The $\alpha6\beta3\gamma2L$ GABAR currents displayed maximal inhibition of 32 ± 9% ($n = 7$, $p < 0.003$) at 3 mM lanthanum with an $IC_{50}$ value of 117 ± 32 $\mu$M and Hill slope of −1.1, and the $\alpha6\beta3\delta$ GABAR currents showed maximal inhibition of 83 ± 4% ($n = 7$; $p < 0.000007$) at 600 $\mu$M lanthanum with and $IC_{50}$ value of 29 ± 6 $\mu$M and Hill slope of −1.3 (Fig. 2, B and C).

The potentiation of $\alpha1\beta3\gamma2L$ GABA currents was, however, lower at 3 mM lanthanum compared with that at 1 mM lanthanum [141 ± 9% ($n = 8$, $p < 0.003$) and 164 ± 11% of control current, respectively]. At higher concentrations of lanthanum, there was no significant potentiation or inhibition of the current in the presence of lanthanum as compared with the control current in the absence of lanthanum. The average currents in the presence of 6 and 10 mM lanthanum were 97 ± 11% ($n = 3$, $p = 0.8$) and 87 ± 16% ($n = 3$, $p = 0.5$) of the control current, respectively. This suggested that $\alpha1\beta3\gamma2L$ GABA currents were potentiated only at concentrations of lanthanum below 1 mM. At concentrations higher than 1 mM, the potentiating effect of lanthanum decreased, and at 10 mM lanthanum, the $\alpha1\beta3\gamma2L$ GABA current approached the control current in the absence of lanthanum. The decrease in potentiation of $\alpha1\beta3\gamma2L$ GABAR currents occurred at concentrations of lanthanum higher than 1 mM with an $IC_{50}$ value (for the decrease in potentiation) of 4.3 ± 0.6 mM and a Hill slope of −3.8.

**Competitive interaction between lanthanum ions and GABAR isoforms.** To elucidate the mechanism of potentiation and inhibition of different GABAR isoforms by lanthanum, GABA concentration response curves were compared in the absence and presence of the corresponding $EC_{50}$ and $IC_{50}$ values of lanthanum for each of the three GABAR isoforms. The current amplitudes in the absence and presence of lanthanum were normalized to the maximum current evoked by GABA in the absence of lanthanum. The data were fitted by the logistic equation described in Materials and Methods. In the presence of 300 $\mu$M lanthanum, the concentration response curve for $\alpha1\beta3\gamma2L$ GABARs was shifted to lower concentrations of GABA with no increase in the maximum current evoked by GABA (Fig. 3A). The $EC_{50}$ value for GABA in the absence of lanthanum was 13 ± 3.3 $\mu$M and the Hill slope was 1.5 ± 0.1 ($n = 4$). In the presence of 300 $\mu$M lanthanum, the $EC_{50}$ value for GABA was decreased to 6.4 ± 3 $\mu$M and the Hill slope was not significantly changed at 2.0 ± 0.2 ($n = 4$). The decrease in $EC_{50}$ value for GABA was statistically significant ($p = 0.01$) using paired Student's $t$ test, and the Hill slope was not changed significantly ($p = 0.18$). Therefore, lanthanum decreased the GABA $EC_{50}$ value for $\alpha1\beta3\gamma2L$ GABARs without changing the maximum current, suggesting that lanthanum increased the affinity of GABA for the $\alpha1\beta3\gamma2L$ GABARs without changing the number of functional receptors. Unlike the $\alpha1\beta3\gamma2L$ GABAR isoform, concentration response curves for the $\alpha6\beta3\gamma2L$ and $\alpha6\beta3\delta$ GABAR isoforms were shifted to higher concentrations of GABA in the presence of lanthanum with no decrease in the maximum GABA-evoked current. The increases in $EC_{50}$ value for GABA were statistically significant ($p < 0.05$). The $EC_{50}$ value for GABA was increased from 2.5 ± 0.2 $\mu$M to 4.4 ± 0.1 $\mu$M GABA in the presence of 100 $\mu$M lanthanum ($p = 0.004$, $n = 4$) for the $\alpha6\beta3\gamma2L$ GABAR isoform (Fig. 3B), and the $EC_{50}$ value for $\alpha6\beta3\delta$ GABAR isoform was increased from 0.38 ± 0.05 $\mu$M to 1.06 ± 0.23 $\mu$M GABA in the presence of 30 $\mu$M lanthanum ($p = 0.04$, $n = 5$) (Fig. 3C). The Hill slope for $\alpha6\beta3\gamma2L$ GABAR currents was decreased from 1.48 ± 0.09 to 1.22 ± 0.09 ($p = 0.003$, $n = 4$), and that for $\alpha6\beta3\delta$ GABAR currents was altered from 1.22 ± 0.15 to 1.15 ± 0.17 ($p = 0.8$, $n = 5$). Therefore, lanthanum decreased the GABA affinity for the $\alpha6\beta3\gamma2L$ and $\alpha6\beta3\delta$ GABAR isoforms without altering the number of active receptors.

**Voltage independence of the effect of lanthanum on different GABAR isoforms.** To gain some insight regarding the location of the site of interaction between lanthanum and GABAR chloride channel, the voltage dependence of

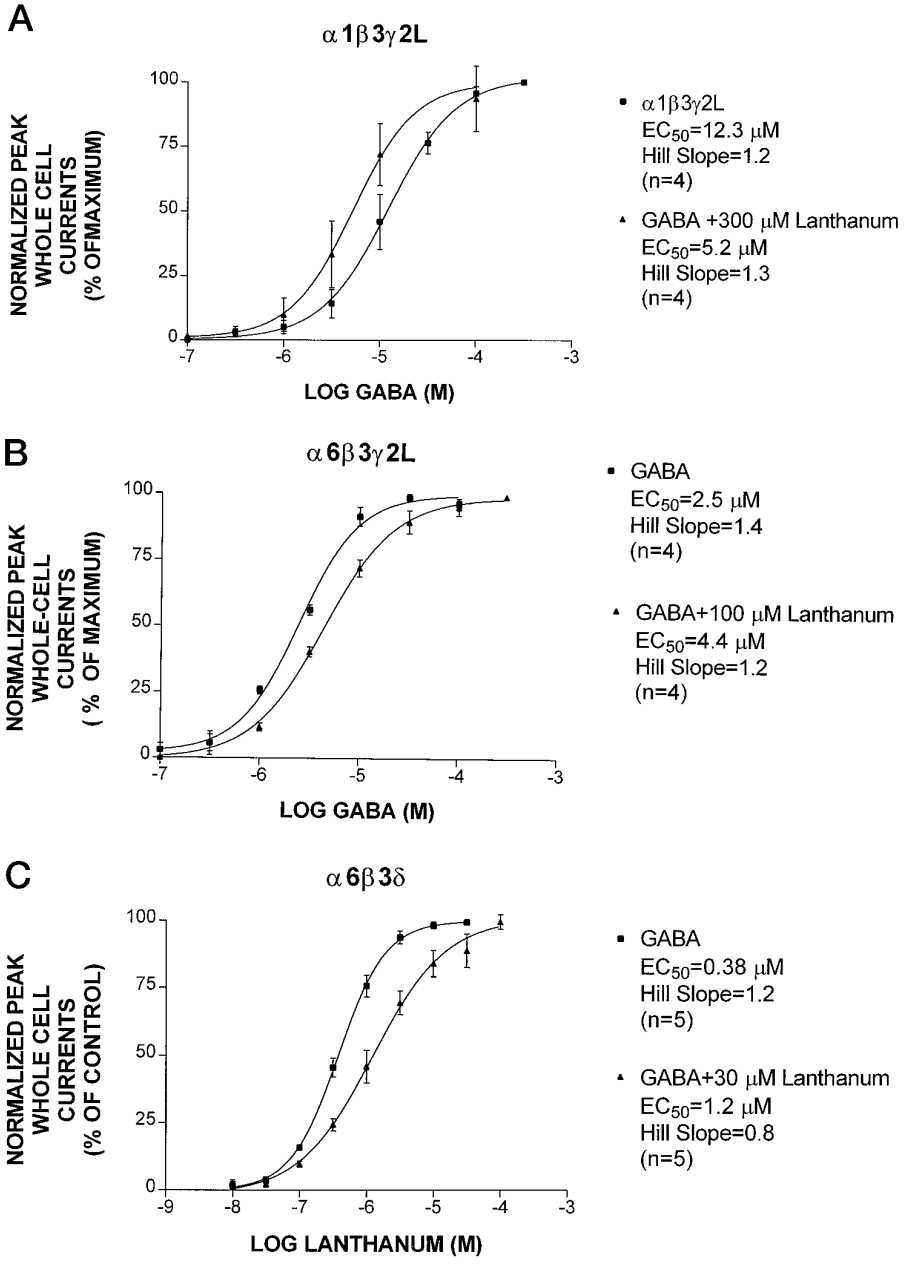


**Fig. 3.** Competition curves for GABA and lanthanum for $\alpha1\beta3\gamma2L$, $\alpha6\beta3\gamma2L$, and $\alpha6\beta3\delta$ GABAR isoforms. Concentration response curves for GABA were obtained in the absence and presence of 300 $\mu$M lanthanum ($\alpha1\beta3\gamma2L$; A), 100 $\mu$M lanthanum ($\alpha6\beta3\gamma2L$; B), and 30 $\mu$M lanthanum ($\alpha6\beta3\delta$; C). *Symbols*, mean values ($n = 3$) of currents normalized to the maximum current evoked in the absence of lanthanum from three cells each for each of the three different isoforms. *Vertical bars*, mean $\pm$ standard error.

GABAR currents was examined in the presence and absence of lanthanum (Fig. 4). The current-voltage relationship in the presence of GABA alone was largely linear for the $\alpha1\beta3\gamma2L$ and $\alpha6\beta3\gamma2L$ isoforms (Fig. 4, A and B) with reversal potentials of 0 and $-6$ mV, respectively, and it showed some departure from linearity for the $\alpha6\beta3\delta$ isoform with a reversal potential of $+5$ mV (Fig. 4C). The average values of the reversal potentials for the three isoforms in the absence and presence of lanthanum were 4.3 $\pm$ 2.4 and 4.9 $\pm$ 1.4 mV ($\alpha1\beta3\gamma2L$, $n = 6$, $p = 0.7$), $-2.0 \pm 2.4$ and $-2.5 \pm 2.0$ mV ($\alpha6\beta3\gamma2L$, $n = 6$, $p = 0.8$) and 3.8 $\pm$ 0.3 and 5.7 $\pm$ 2.5 mV ($\alpha6\beta3\delta$, $n = 5$, $p = 0.5$), respectively. There was no change in the current-voltage relationship in the presence of lanthanum for any of the three GABAR isoforms studied, consistent with voltage-independent potentiation and inhibition by lanthanum.

## Discussion

**Subunit-dependent inhibition and potentiation of different GABAR isoforms by lanthanum.** In contrast to the mainly inhibitory effects of divalent cations, the trivalent cation lanthanum has been shown to enhance GABAR currents in rat DRG neurons (2) and in recombinant $\alpha1\beta2$ and $\alpha1\beta2\gamma2$ GABARs expressed in human embryonic kidney (A293) cells (3). Reichling and MacDermott (1) reported a biphasic effect of lanthanum on rat dorsal horn neurons: at concentrations between 1 and 100 $\mu$M, lanthanum-enhanced GABAR currents to a maximum of 130% of control, whereas at higher concentrations, lanthanum markedly reduced GABAR currents (1).

The present study further clarifies the interactions between lanthanum and GABARs by demonstrating contrast-

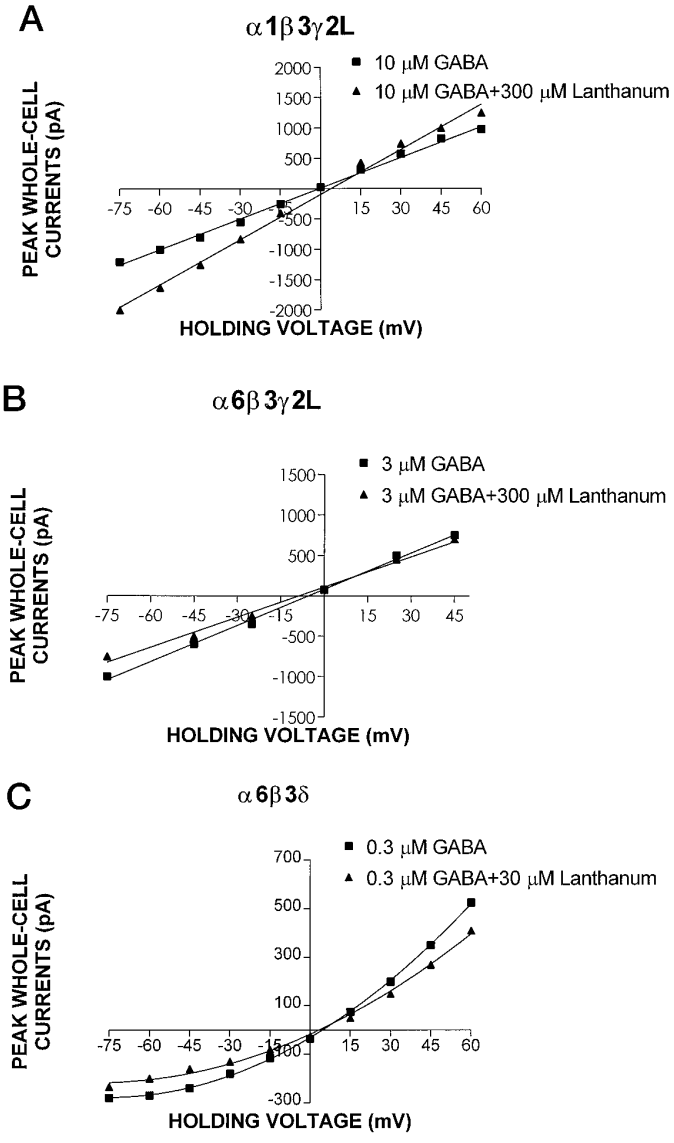


**Fig. 4.** Current-voltage relationships for $\alpha1\beta3\gamma2L$, $\alpha6\beta3\gamma2L$, and $\alpha6\beta3\delta$ GABAR isoforms in the absence and presence of lanthanum. Representative current-voltage curves for GABA currents evoked in the absence and presence of lanthanum are shown for $\alpha1\beta3\gamma2L$ (10 $\mu$M GABA+300 $\mu$M lanthanum; A), $\alpha6\beta3\gamma2L$ (3 $\mu$M GABA+100 $\mu$M lanthanum; B), and $\alpha6\beta3\delta$ (0.3 $\mu$M GABA+30 $\mu$M lanthanum; C) GABAR isoforms. Step changes in holding voltage were applied for voltages ranging from −75 mV to +60 mV.

ing actions, inhibition and potentiation, of lanthanum on different recombinant GABARs and by adding a structural basis to the distinctive actions of lanthanum on GABARs, which suggest that changing the $\alpha$-subunit subtype from $\alpha1$ to $\alpha6$ alters the effect of lanthanum on GABARs from potentiation to inhibition at comparable (micromolar) concentrations of lanthanum. It further suggests that the level of maximal inhibition of GABAR currents by lanthanum in $\alpha6$-containing GABAR isoforms is greater in the presence of the $\delta$ subunit (83%) than in the presence of a $\gamma$ subunit (32%), probably due to a greater shift in the $EC_{50}$ value for GABA in $\delta$-containing receptors (3-fold; 0.38 to 1.2 $\mu$M) compared with $\gamma$-containing receptors (2-fold; 2.5 to 4.4 $\mu$M). Comparison of the modulatory effects of 100 $\mu$M lanthanum on the three different GABAR isoforms demonstrated its contrasting actions, showing distinct potentiation of $\alpha1\beta3\gamma2L$ GABAR currents ($20 \pm 7\%$, $n = 8$, $p = 0.026$), marked inhibition of $\alpha6\beta3\delta$ GABAR currents ($71 \pm 4\%$, $n = 8$, $p < 0.0003$), and weak inhibition of $\alpha6\beta3\gamma2L$ GABAR currents ($19 \pm 8\%$, $n = 8$, $p < 0.0002$). Therefore, the structural change associated with the presence of the $\alpha1$ subtype instead of the $\alpha6$ subunit resulted in a functional change from inhibition to potentiation by lanthanum, whereas the change associated with the presence of the $\delta$ instead of the $\gamma$ subunit resulted in increased maximal inhibition by lanthanum. This could explain, at least in part, reports of biphasic effects of lanthanum on GABAR currents (1) and the lack thereof (2) because the manifestation of the biphasic effects of lanthanum would depend on the differences in composition of functional GABAR isoforms present in the different regions studied (dorsal horn versus dorsal root ganglion neurons), their relative abundance, and the concentration of GABA (100 $\mu$M versus 10 $\mu$M) studied. The loss of potentiation of $\alpha1\beta3\gamma2L$ GABAR currents by lanthanum at concentrations above 1 mM also could underlie the manifestation of biphasic effects of lanthanum on GABAR currents in dorsal horn neurons (1). In the presence of both $\alpha1\beta3\gamma2L$ and $\alpha6\beta3\delta$-like GABAR isoforms, it is conceivable that, at lower concentrations of lanthanum (0.1 to 100 $\mu$M), the enhancing effect of lanthanum could dominate, whereas at higher concentrations of lanthanum (300 $\mu$M to 3 mM), loss of potentiation of the $\alpha1\beta3\gamma2L$-like isoform by lanthanum could result in unmasking of the inhibitory effect of lanthanum on the $\alpha6\beta3\delta$-like isoform. This corresponds well with the maximum potentiation (35%) and inhibition (80%) of GABA-evoked currents and the corresponding concentrations of lanthanum (30 $\mu$M and 3 mM, respectively) at which the effects occurred, in the biphasic response seen in dorsal horn neurons by Reichling and MacDermott (1). Region-specific distribution of different GABAR subunit mRNAs has been demonstrated in the rat brain (21, 22), whereas immunoprecipitation studies have revealed the presence of specific GABAR isoforms in the rat cerebellum and cerebral cortex (23–25). Recent immunohistochemical analysis of GABAR heterogeneity in rat spinal cord also showed colocalization of different subunit subtypes in distinct laminar compartments (26). Although $\alpha6$ and $\delta$ subunits could not be detected in the spinal cord, $\alpha1$, $\alpha2$, and $\alpha5$ subunit subtypes showed restricted, lamina-specific distribution whereas the $\alpha3$ subtype showed widespread expression. Therefore, region-specific expression of different GABAR isoforms composed of different $\alpha$ subunit subtypes in the presence or absence of $\gamma$ or $\delta$ subunits in the dorsal horn versus dorsal root ganglion neurons could underlie the differences in the observed effects of lanthanum between the two studies.

This study also indicates that the presence of the $\delta$ subunit increases the efficacy of inhibition of GABAR currents by lanthanum, implying a correlation between the structural change represented by $\delta$ subunit instead of $\gamma$ subunit and the functional change in inhibition of GABAR currents from 83% in $\delta$-containing GABAR isoforms to 32% in $\gamma$-containing GABAR isoforms. Although not identical, this is consistent with our report of no significant potentiation of $\alpha1\beta1\delta$ isoform by lanthanum (300 $\mu$M lanthanum) and distinct potentiation by lanthanum of the $\alpha1\beta1$ isoform (27). The structural determinant of lanthanum potentiation contributed by the $\alpha1$ subunit in the $\alpha1\beta1$ GABARs could be countered by a reverse contribution from the $\delta$ subunit in the $\alpha1\beta1\delta$ isoform, giving

rise to the lack of effect of lanthanum seen in the $\alpha1\beta1\delta$ isoform. However, this result must be interpreted with caution because the effect of lanthanum on GABAR currents was studied at single, specific concentrations of lanthanum (300 $\mu$M) and GABA (10 $\mu$M). Moreover, due to the low efficiency of expression of $\alpha6\beta3$ GABARs in our expression system (20), we could not compare the action of lanthanum on $\alpha6\beta3$ GABARs with those on $\alpha6\beta3\delta$ and $\alpha6\beta3\gamma2L$ GABARs to provide further evidence for this hypothesis. The presence of different subtypes of the $\beta$ subunit ($\beta1$ versus $\beta3$) also could potentially play a role in determining the effect of lanthanum on different GABAR isoforms. Knowledge of subunit selectivity of lanthanum could be instrumental in characterizing the molecular properties of GABARs and in understanding the regional and developmental diversity of neuronal GABARs.

**Extracellular location of site for lanthanum interaction.** Results from the present study suggest that the site of interaction with lanthanum lies on the extracellular surface of GABARs. First, the quick onset and removal of the effect of lanthanum during acute application (5-sec pulses) of lanthanum in the whole-cell recording configuration suggests that the action is mediated by an extracellular event. Second, the competitive nature of potentiation and inhibition by lanthanum with respect to GABA also suggests that the site of interaction between GABARs and lanthanum is likely to be extracellular. Third, the lack of a clear voltage dependence in the current-voltage relationship in the presence of lanthanum as compared with that in its absence also suggests that the site for lanthanum interaction sensed little or none of the transmembrane electrical gradient and, therefore, was likely to be extracellular. Earlier work by Ma and Narahashi (2) also suggested that the potentiation by lanthanum was nearly voltage independent, whereas that of Im *et al.* (3) suggested weak voltage dependence. Based on our results, the extracellular lanthanum interaction site on GABAR is subject to characteristic functional modulation by the $\alpha$-subunit subtype (potentiation versus inhibition) and the $\gamma/\delta$ subunits (extent of inhibition) and, therefore, might be composed mainly of contributions from the extracellular regions of at least the $\alpha$ and $\gamma/\delta$ subunits.

**Physiological implications of enhancement and inhibition of distinct GABAR isoforms by lanthanum.** Potentiation of the $\alpha1$-containing and inhibition of the $\alpha6$-containing (putative) cerebellar GABAR isoforms by lanthanum might increase the plasticity of the cerebellum from a therapeutic or functional perspective. GABAergic neurotransmission has been proposed to play an important role in the perception of pain. Selective depression of noxiously evoked activity from rat and feline spinal cord neurons by intravenous injection of midazolam and clinical control of pain by subarachnoid infusion of midazolam have been reported (28–30). It has been postulated that pain perception is modulated in the substantia gelatinosa (lamina II), which controls impulse transmission from the primary afferents to projecting neurons (31, 32). By demonstrating a striking segregation of distinct GABAR subunits in functionally different neuron populations in the substantia gelatinosa ($\alpha2$, $\alpha3$) and in projecting neurons ($\alpha1$), Bohlhalter *et al.* (26) have suggested differential modulation of GABAergic neurotransmission by specific pharmacological agents and pharmacological control of nociception and treatment of neurogenic pain based on $GABA_A$ receptor heterogeneity in the future. Lanthanum administered into the lumbar subarachnoid space of rat has been shown to have antinociceptive effects (33). Based on the subunit-specific modulation of GABAR currents by lanthanum described in the present study, lanthanum could be an important resource in the functional characterization of GABAR isoforms in the substantia gelatinosa and projecting neurons ultimately providing insights into the role of receptor heterogeneity in signal processing and mechanisms of pain.

Based on the increasingly diverse applications of lanthanum-containing compounds in industry and therapeutics (5), the distinct actions of lanthanum on different GABAR isoforms offer potential tools to understand the structural and functional diversity of GABARs in nature and to envision more receptor-specific targeting of drugs in pathophysiological situations.

**References**


1. Reichling, D. B., and A. MacDermott. Lanthanum actions on excitatory amino acid-gated currents and voltage-activated $Ca^{2+}$ currents in rat dorsal horn neurons. *J. Physiol.* **441:**199–218 (1991).
2. Ma, J. Y., and T. Narahashi. Differential modulation of $GABA_A$ receptor-channel complex by polyvalent cations in rat dorsal root ganglion neurons. *Brain Res.* **607:**222–232 (1993).
3. Im, M. S., B. J. Hamilton, D. B. Carter, and W. B. Im. Selective potentiation of GABA-mediated $Cl^-$ current by lanthanum ion in subtypes of cloned $GABA_A$ receptors. *Neurosci. Lett.* **144:**165–168 (1992).
4. Narahashi, T., J. Y. Ma, O, Arakawa, E. Reuveny, and M. Nakahiro. GABA receptor-channel complex as a target site of mercury, copper, zinc and lanthanides. *Cell. Mol. Neurobiol.* **14:**599–621 (1994).
5. Das, T., A. Sharma, and G. Talukder. Effects of lanthanum in cellular systems. A review. *Biol. Trace Elem. Res.* **18:**201–228 (1988).
6. Haley, T. J. Pharmacology, and toxicology of the rare earth elements. *J. Pharm. Sci.* **54:**663–670 (1965).
7. Palmer, R. J., J. L. Butenhoff, and J. B. Stevens. Cytotoxicity of the rare earth metals cerium, lanthanum, and neodymium in vitro: comparisons with cadmium in a pulmonary macrophage primary culture system. *Environ. Res.* **43:**142–156 (1987).
8. Venogopal, B., and T. D. Luckey. *Metal Toxicity in Mammals*. Vol. 2. Plenum Press, New York, 135 (1980).
9. Macdonald, R. L., and R. W. Olsen. $GABA_A$ receptor channels. *Annu. Rev. Neurosci.* **17:**569–602 (1994).
10. Kozak, M. Possible role of flanking nucleotides in recognition of the AUG initiator codon by eukaryotic ribosomes. *Nucleic Acids Res.* **9:**5233–5262 (1981).
11. Kozak, M. Compilation and analysis of sequences upstream from the translational start site in eukaryotic mRNAs. *Nucleic Acids Res.* **12:**857–872 (1984).
12. Hugenvik, J. I., M. W. Collard, R. E. Stofko, A. F. Seasholtz, and M. D. Uhler. Regulation of the human enkephalin promoter by the two isoforms of the catalytic subunit of cyclic adenosine 3′,5′-monophosphate-dependent protein kinase. *Mol. Endocrinol.* **5:**921–930 (1991).
13. Hall, C. V., P. E. Jacob, G. M. Ringold, and F. Lee. Expression and regulation of *Escherichia coli lac Z* gene fusions in mammalian cells. *J. Mol. Appl. Genet.* **2:**101–109 (1983).
14. Chen, C., and H. Okayama. High efficiency transformation of mammalian cells by plasmid DNA. *Mol. Cell Biol.* **7:**2745–2752 (1987).
15. Sanes, J. R., J. L. R. Rubenstein, and J. F. Nicolas. Use of a recombinant retrovirus to study post-implantation cell lineage in mouse embryos. *EMBO J.* **5:**3133–3142 (1986).
16. Nolan, G. P., S. Fiering, J. F. Nicolas, and L. A. Herzenberg. Fluorescence-activated cell analysis and sorting of viable mammalian cells based on $\beta$-D-galactosidase activity after transduction of *Escherichia coli lacZ*. *Proc. Natl. Acad. Sci. USA* **85:**2603–2607 (1988).
17. Greenfield L. J., and R. L. Macdonald. Whole-cell and single-channel $\alpha1\beta1\gamma2S$ GABAA receptor currents elicited by a "multi-puffer" drug application device. *Pfluegers Arch. Eur. J. Physiol.* **432:**1080–1090 (1996).
18. Macdonald, R. L., C. J. Rogers, and R. E. Twyman. Kinetic properties of $GABA_A$ receptor main conductance state of mouse spinal cord neurones in culture. *J. Physiol. (Lond.)* **410:**479–499 (1989).
19. Porter, N. M., R. E. Twyman, M. D. Uhler, and R. L. Macdonald. Cyclic AMP-dependent protein kinase decreases $GABA_A$ receptor current in mouse spinal cord neurons. *Neuron* **5:**789–796 (1990).
20. Saxena, N. C., and R. L. Macdonald. Properties of putative cerebellar $\gamma$-aminobutyric $acid_A$ receptor isoforms. *Mol. Pharmacol.* **49:**567–579 (1996).
21. Laurie, D. J., P. H. Seeburg, and W. Wisden. The distribution of 13 $GABA_A$ receptor subunit mRNAs in the rat brain. II. Olfactory bulb and cerebellum. *J. Neurosci.* **12:**1063–1076 (1992).

22. Wisden, W., D. J. Laurie, H. Monyer, and P. H. Seeburg. The distribution of 13 $GABA_A$ receptor subunit messenger RNAs in the rat brain. I. Telencephalon, diencephalon, mesencephalon. *J. Neurosci.* **12:**1040–1062 (1992).
23. Quirk, K., N. P. Gillard, C. I. Ragan, P. J. Whiting, and R. M. McKernan. Model of subunit composition of γ-aminobutyric acid-A receptor subtypes expressed in rat cerebellum with respect to their α and δ subunits. *J. Biol. Chem.* **269:**16020–16028 (1994).
24. Khan, Z. U., A. Gutierrez, and A. L. De Blas. The subunit composition of a $GABA_A$/benzodiazepine receptor from rat cerebellum. *J. Neurochem.* **63:**371–374 (1994).
25. Pollard, S., M. J. Duggan, and F. A. Stephenson. Further evidence for the existence of α subunit heterogeneity within discrete γ-aminobutyric $acid_A$ receptor subpopulations. *J. Biol. Chem.* **268:**3753–3757 (1993).
26. Bohlhalter S., O. Weinmann, H. Mohler, and J.-M. Fritschy. Laminar compartmentalization of $GABA_A$-receptor subtypes in the spinal cord: an immunohistochemical study. *J. Neurosci.* **16:**283–297 (1996).
27. Saxena, N. C., and R. L. Macdonald. Assembly of $GABA_A$ receptor subunits: role of the δ subunit. *J. Neurosci.* **14:**7077–7086 (1994).
28. Clavier, N., M. Lombard, and J. Besson. Benzodiazepines and pain: effects of midazolam on the activities of nociceptive non-specific dorsal horn neurons in the rat spinal cord. *Pain* **48:**61–71 (1992).
29. Sumida, T., M. Tagami, Y. Ide, M. Nagase, H. Sekiyama, and K. Hanaoka. Intravenous midazolam suppresses noxiously evoked activity of spinal wide dynamic range neurons in cats. *Anesth. Analg.* **80:**58–63 (1995).
30. Schoeffler, P., P. Auroy, J. E. Bazin, J. Taxi, and A. Woda. Subarachnoid midazolam: histologic study in rats and report of its effect on chronic pain in humans. *Reg. Anesth.* **16:**329–332 (1991).
31. Melzack, R., and P. D. Wall. Pain mechanism: a new theory. *Science (Washington D. C.)* **150:**971–979 (1965).
32. Wall, P. D. The substantia gelatinosa. A gate control mechanism set across sensory pathway. *Trends Neurosci.* **3:**221–224 (1990).
33. Reddy, S. V. R., and T. L. Yaksh. Antinociceptive effects of lanthanum neodymium and europium following intrathecal administration. *Neuropharmacology* **19:**181–185 (1980).

**Send reprint requests to:** Dr. Robert L. Macdonald, Neuroscience Laboratory Building, 1103 East Huron Street, Ann Arbor, MI 48104-1687.